

Order from Disorder in the Two-Dimensional Kondo-Necklace

Wolfram Brenig

Technische Universität Braunschweig, Mendelssohnstr. 3, 38106 Braunschweig, Germany

(Dated: 23rd March 2024)

We analyze the effects of site-dilution disorder on the thermodynamic properties of the two-dimensional Kondo necklace using finite-temperature stochastic series expansion. Results will be discussed for the dependence on dilution concentration, temperature, and Kondo exchange-coupling strength of the uniform susceptibility, the staggered structure factor, and the Chakravarty-Halperin-Nelson ratio. Dilution is shown to induce effective free-spin clusters in the gapped phase of the clean system with a low-temperature Curie constant renormalized below $1/4$. Furthermore, dilution is demonstrated to generate antiferromagnetic order in the quantum disordered phase of the clean system, i.e. order-from-disorder. In turn, the quantum critical point of the clean system, separating an antiferromagnetic from a paramagnetic dimerized state at a critical Kondo exchange-coupling strength $J_c = 1/4$ is suppressed. Finally, speculations on a renormalized classical behavior in the dilution induced ordered phase are stated.

PACS numbers: 75.10.Jm, 05.70.Jk, 75.40.Cx, 75.40.Mg

Quantum critical points (QCPs), i.e. zero temperature phase transitions as a function of some control parameter are likely to be at the core of unconventional finite temperature behavior of many novel materials^{1,2}. Quantum antiferromagnets (AFMs) with an intrinsic spin dimerization and weak inter-dimer exchange like $K(Tl)CuCl_3$ ^{3,4} or $BaCuSi_2O_6$ ⁵ are of particular interest here, since they allow for switching between quantum disordered spin-gapped phases and states with magnetic long-range order (LRO). QCPs have been induced in these materials both, by tuning the inter-dimer exchange via pressure^{6,7,8}, as well as by applying external magnetic fields^{9,10,11}.

Combining the physics of quantum critical spin systems with that of disorder is an open issue. Site dilution with non-magnetic impurities has been observed to induce LRO in the spin gapped phases of several dimerized quantum AFMs^{12,13,14,15}. In spin ladders and dimerized spin chains a picture of weakly interacting 'defect moments' has emerged with enhanced AFM correlations in the vicinity of the non-magnetic sites^{16,17,18,19}. In dimensions $D = 2$ and at finite impurity concentration this may trigger LRO in spin-gapped systems on bipartite lattices and remove a QCP²⁰. In the context of the cuprate parent compounds²¹, site dilution of the 2D Heisenberg AFM has been shown to lead to a QCP at percolation where LRO is suppressed^{22,23}. In addition to site dilution several other forms of disorder are of interest. Early on random exchange has been investigated in a variety of 1D and 2D Heisenberg and Ising AFMs where it can lead to random singlet fix-points^{24,25,26} and Griffiths phases²⁷. Very recently 'dimer dilution' has been studied in bi-layer Heisenberg models yielding multicritical points at percolation^{28,29,30}.

In this work we focus on random site dilution in the $SU(2)$ symmetric 2D spin-1/2 Kondo-necklace (SKN) which is shown in fig. 1

$$H_{SKN} = \sum_{lm} j \sum_{\mathbf{l}} S_{P\mathbf{l}} \cdot S_{m\mathbf{l}} + \sum_{\mathbf{l}} J \sum_{\mathbf{l}} S_{P\mathbf{l}} \cdot S_{I\mathbf{l}} \quad (1)$$

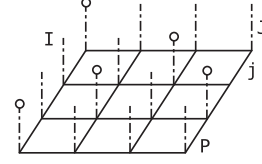


Figure 1: 2D Kondo-necklace. Spin-1/2 moments coupled by j and J and located at vertices in 'conduction-plane' P and on 'Kondo-sites' in plane I at end of dash-dotted lines. ' \circ ' labels randomly diluted 'Kondo-sites' with no magnetic moment.

with $j = 1$ hereafter. This model can be viewed as the strong coupling limit at large Coulomb correlations in the conduction electron band of the Kondo-lattice model at half filling³¹. In turn, the two layers P and I in fig. 1, will be loosely referred to as 'conduction-band' and 'Kondo-site' layer hereafter. The clean limit of the 2D SKN has been studied at finite temperatures recently^{31,32}. The model exhibits a QCP between AFM-LRO and a dimer phase at $J_c = 1/4$. It shows temperature-scaling and a Chakravarty-Halperin-Nelson ratio consistent with the $O(3)$ non-linear sigma model. The aim of this work is to shed light onto the effect of randomly substituting non-magnetic ions into the Kondo-layer, as shown in fig. 1. In that case the site index l in the second sum of eqn. (1) runs only over those sites which are *occupied by a spin* in layer I .

Our analysis is based on the stochastic series expansion (SSE) with loop-updates introduced by Sandvik and Syljuasen^{33,34}. Averaging over disorder configurations is performed by rapid thermalization using the temperature-halving scheme proposed by Sandvik³⁵. We refer the reader to the latter three references for details. In the following, all of the SSE results reported for a finite dilution concentration comprise of an average over 1000 disorder configurations on a system of $N = 24 \times 24 \times 2$ sites. The latter is justified by the rather weak finite size dependence observed beyond this for the clean system³¹.

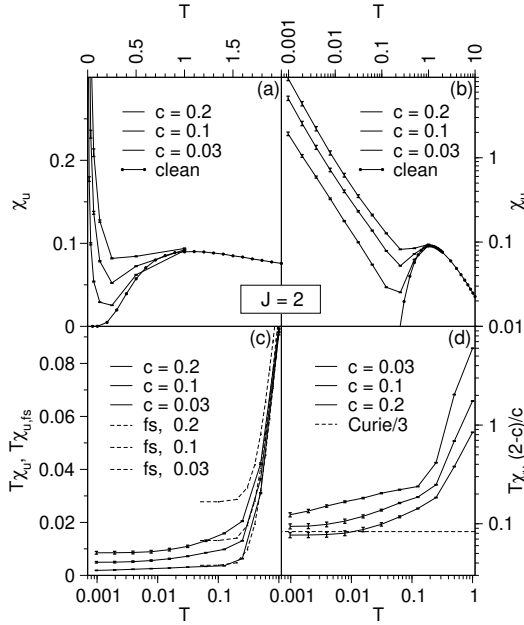


Figure 2: (a), (b): Uniform susceptibility χ_u at $J = 2 > J_c$ vs. temperature for $c=0.03, 0.1$ and 0.2 and $1=1024$ $T = 1$ and for $c = 0$ and 0.05 $T = 1$ on a lin-lin (a) and a log-log scale (b). (c): $T\chi_u$ product at $c \neq 0$ as compared with 'free spin' approximation $T\chi_{u,fs}$ from eqn. (3), for identical parameters as in (a). (d): $T\chi_u$ product at $c \neq 0$ as compared to Curie behavior renormalized by $1/3$. Statistical errors in all panels either less than the solid-circle marker size or depicted by error bars. Legends label plots from top to bottom.

To begin we discuss the uniform susceptibility

$$\chi_u = m^2 / T; \quad (2)$$

where T is the temperature and $m = \frac{1}{N} \sum_{n=P+1}^P S_{n1}^z = N^\circ$ is the total spin z -component with N° being the total number of sites *occupied* by a spin. The defect concentration is $c = 2N^\circ / N$, where N° is the number of empty site in layer I , i.e. $N^\circ = (2 - c)N/2$. In fig. 2 we summarize several aspects of χ_u versus temperature at $J > J_c$ which refers to the gapped phase of the clean system. The figure contrasts the clean system for $0.05 < T < 1$ against three impurity concentrations $c = 0.03, 0.1$, and 0.2 for $1=1024$ $T = 1$. First, fig. 2(a) clearly demonstrates that the non-magnetic defects induce low-energy magnetic density of states in the spin gap. Second, the log-log plot of fig. 2(b) shows, that the susceptibility of these states is similar to that of 'free' spins, i.e. it follows almost a Curie law in the temperature range below the spin gap.

To further elucidate the free spin behavior, we start from the strong coupling limit, i.e. $J \gg 1$, of the Kondo-necklace. In that case and in the clean system the ground state is a product of singlets on the dash-dotted bonds of fig. 1. Removing a 'Kondo' spin leaves a free spin in the 'conduction' plane. Denoting the uniform susceptibility per occupied site by $\chi_{u,fs}$, with the index fs referring to

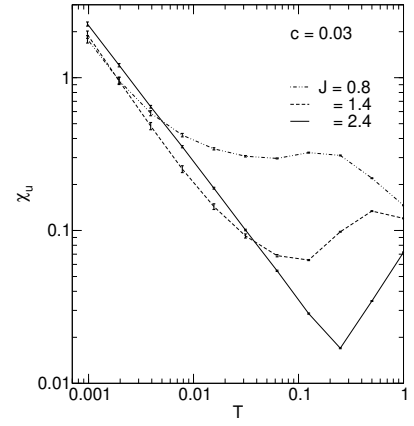


Figure 3: Uniform susceptibility χ_u vs. temperature at $c = 0.03$ for $J = 0.8$ (dashed-double-dotted), 1.4 (dashed), and 2.4 (solid), corresponding to the AFM-LRO, the critical and the gapped regime at $c = 0$. Statistical errors are depicted by vertical bars.

the free spins, one has

$$\chi_{u,fs} = \frac{2(1-c)}{(2-c)} \chi_u(c=0) + \frac{c}{(2-c)} \frac{1}{4T}; \quad (3)$$

The first term is the contribution from the singlets and the second term stems from the free spins. To assess the relevance of this free spin picture - other than in the strong coupling limit - we may use eqn. (3) with $\chi_u(c=0)$ taken from the SSE at $c=0$ but for J other than 1 . In fig. 2(c) $T\chi_{u,fs}$ from this approximation is compared with $T\chi_u$ from eqn.(2) at $J = 2$. First, at low temperatures $T\chi_u$ is smaller than $T\chi_{u,fs}$. Second, while $T\chi_{u,fs}$ saturates on an energy scale set by the spin gap, $T\chi_u$ continues to decrease as a function of T and seem to saturate at far lower temperatures. This is a clear indication of low-energy correlations which develop between the impurity induced degrees of freedom. This also clarifies the need for SSE results at far lower values of T at finite disorder as compared to the clean case.

For site diluted spin-ladders Sigrist and Furusaki have proposed¹⁷ that below a crossover temperature, and due to long-range, higher order exchange the free spins will form clusters of a size set by the inverse temperature. These clusters lead to a Curie-type of susceptibility per defect, however with a Curie constant reduced from $1/4$ to $1/(3-4)$. The argument of ref.¹⁷ is not restricted to ladders. To consider this, fig. 2(d) shows the Curie contribution normalized to the defect concentration on a log-log scale. For $c < 0.1$ saturation of $T\chi_u$ can be anticipated for $T < 1=500$. Consistently with ref.¹⁷ $\lim_{T \rightarrow 0} [T\chi_u(2-c)/c] < 1/4$. Moreover, while a renormalization by a factor of exactly $1/3$ can not be read off from this figure, the reduction is very close to this value. The kink in $T\chi_u$ observable at elevated temperatures and small concentrations in this log-log plot is related to the opening of the spin gap.

Fig. 3 clarifies the difference between the gapped and

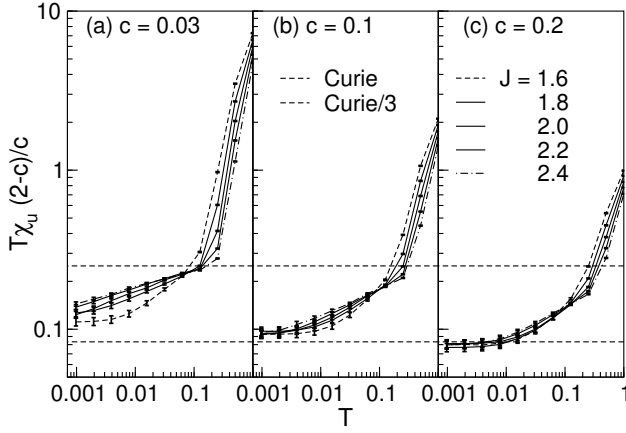


Figure 4: T_u vs. T at $c = 0.03$ (a), 0.1 (b), and 0.2 (c) for various values of $J > J_c$. Dashed straight lines correspond to (renormalized) Curie constant. Legends label plots according to order listed between dashed and dashed-dotted. Statistical errors are depicted by vertical bars.

the ordered phase as well as the impact of finite size gaps. In contrast to the gapped phase, site dilution of the LRO phase is not expected to induce quasi free moments because of the AFM correlations between all the occupied sites³⁶. On finite systems however, a size-dependent spin gap will remain also in the AFM-LRO phase. Disorder will eventually induce states in this gap, leading to an increase of the uniform susceptibility, however at a temperature scale much lower than and unrelated to J . This is consistent with the results shown for small concentration in fig. 3. In the gapped phase, at $J=2.4$ an almost straight-line behavior can be observed on a log-log scale below an energy set by the intrinsic spin gap. In the LRO phase at $J=0.8$ such behavior can only be anticipated at temperatures at least two orders of magnitude lower.

In fig. 4 we summarize T_u versus T for $c = 0.03, 0.1$, and 0.2 over a finite range of coupling constants J corresponding to the gapped regime of the clean system. First, while low-temperature convergence to a constant T_u is observed for $c = 0.1$ and 0.2 , fig. 4 allows for an approximate extrapolation to $T = 0$ at $c = 0.03$ only. Second, it is tempting to claim that at fixed c the low temperature Curie constant depends only weakly on J . Third, the low temperature Curie constant is less than $1/4$ and close to $1/3$ for all cases depicted. However, the figure suggests that the Curie constant is a *decreasing* function of c and cannot be described by a single renormalization factor at all c . This is consistent with the fact, that at $c = 1$ the SKN is identical to the 2D AFM Heisenberg model, for which $\lim_{T \rightarrow 0} T_u = 0$.

Now we turn to the longitudinal staggered structure factor, i.e. the order parameter for AFM-LRO

$$S(Q) = \frac{D}{m_Q^z} \frac{E}{2}; \quad (4)$$

where $m_Q^z = \frac{1}{N} \sum_{n=P+1}^P S_{n1}^z \exp(iQ \cdot r_n)$ is the staggered magnetization with $Q = (\pi; \pi)$. All results dis-

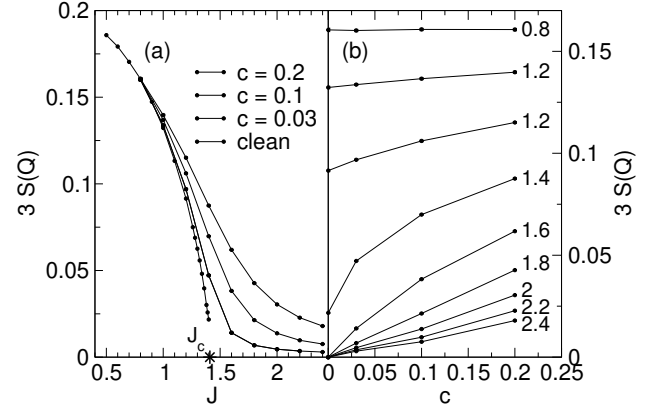


Figure 5: Low-temperature staggered magnetization $3S(Q)$ versus J for various $c = 0, 0.03, 0.1$, and 0.2 (a) and versus c for various $J = 0.8 :: 2.4$ (b). Statistical errors are either less than the solid-circle marker size or are depicted by vertical bars. Legends label plots from top to bottom.

cussed correspond to values of T such that low temperature saturation of $S(Q)$ has been reached. Fig. 5(a) shows the squared staggered moment $M_Q^2 = 3S(Q)$ versus J for the clean case and for $c=0.03, 0.1$ and 0.2 . In the clean case M_Q^2 is finite below the critical value of $J = J_c$ and, apart from finite size effects, drops to zero for $J > J_c$. I.e. J_c corresponds to the QCP³¹ with AFM-LRO for $J < J_c$ and a spin gapped state for $J > J_c$. Generating SSE data of smaller value of M_Q^2 for $J > J_c$ at $c = 0$ requires 'fine-tuning' of J which we refrain from.

The main result of fig. 5(a) is contained in the change of M_Q^2 versus J upon doping. First, for all concentrations investigated the QCP disappears. Second, a finite staggered moment can be observed at all values of J and in particular also in the formerly gapped phase of the clean system. This implies that doping by non magnetic impurities induces AFM-LRO in the quantum disorder phase of the SKN, i.e. *order-from-disorder*. It is tempting to speculate, that this behavior is true for all c .

We may also discuss these results from a different point of view, i.e. by considering M_Q^2 versus the impurity concentration for various exchange coupling constants, as in fig. 5(b). This shows M_Q^2 to increase at small c , both below and above J_c . At J_c the induced AFM order is most sensitive to the impurity concentration. For $c \neq 1$ all curves are expected to join at a single value corresponding to the staggered magnetization of the planar Heisenberg AFM. For $c = 0$ and $J = 1.6 > J_c$, M_Q^2 has been forced to zero in fig. 5(b). This neglects finite size effects, namely that $M_Q^2 \neq 0$, albeit small, even for $c = 0$ since $N = 24$ is finite. In principle this value of M_Q^2 ($J > J_c; c = 0$) can be read off by extrapolating to $c \rightarrow 0$ for each $J > J_c$ in fig. 5(b).

Finally we discuss the Chakravarty-Halperin-Nelson

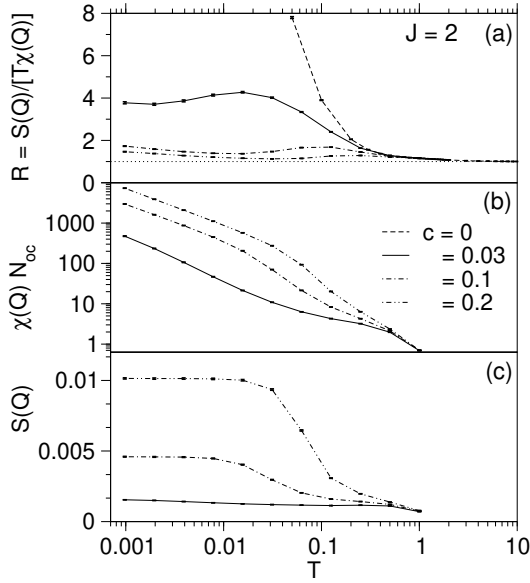


Figure 6: (a): Chakravarty-Halperin-Nelson ratio R of the total staggered structure factor and susceptibility vs. temperature at $J = 2 > J_c$ for $c = 0, 0.03, 0.1$, and 0.2 , corresponding to dashed, solid, dashed-dotted and dashed-double-dotted. Result for $c = 0$ in panel (a) from ref.³¹. Temperatures are $1=1024$ $T = 1$ (0.05 $T = 10$) for $c \in 0$ ($c = 0$). Dotted line: unity. (b) and (c): denominator $\chi(Q)$ and numerator $S(Q)$ from eqn. (5) for R vs. temperature with c as in fig. 6 (a). Size of statistical errors is given by vertical bars in all panels.

ratio

$$R = \frac{S(Q)}{T \chi(Q)} : \quad (5)$$

which, in addition to $S(Q)$ includes information on the longitudinal staggered susceptibility

$$\chi(Q) = \sum_{\mathbf{Q}} \sum_{\mathbf{Q}'} \frac{1}{\Omega} \langle \mathbf{S}_{\mathbf{Q}}^z \mathbf{S}_{\mathbf{Q}'}^z \rangle \quad (6)$$

This ratio relates our analysis to that of the AFM non-linear σ -model (NL σ M)^{1,2,37}. Regarding clean systems with a QCP between AFM-LRO and dimerization, this ratio has been studied in detail for the bilayer Heisenberg AFM³⁸ and for the SKN³¹. In agreement with the NL σ M it was found that $R = 1$ in the (classical) high- T regime, as well as in AFM-LRO (renormalized classical) regime for $T \neq 0$. At the QCP the NL σ M requires $R(T \rightarrow 0) \neq 1$, which is also consistent with SSE at $J = J_c$. While - to our knowledge - rigorous results are absent for a disorder induced AFM-LRO phase, as for $J > J_c$, it is yet tempting to speculate that renormalized classical behavior will re-emerge. Since in the gaped phase of the clean system R diverges as T^{-1} this will lead to drastic variations in R versus c for $J > J_c$. Indeed this is observed in fig. 6(a), where R is shown versus T as c varies from 0 to 0.2. Obviously R decreases markedly with increasing c and almost reaches 1 for $c = 0.1$ and $T = 0.01$. As for $c = 0$ the zero temperature limit of R will be very sensitive to finite size gaps^{31,38}. This may cause the low- T increase seen in this figure, i.e. we speculate that for larger systems $R = 1$ as $T \rightarrow 0$ for all $c \in 0$. This has to be clarified by future analysis. For completeness, fig. 6(b) and (c) relate the cancellation of the factor T in the denominator of R at $c \in 0$ to the temperature dependence of $\chi(Q)$.

Acknowledgements Part of this work has been supported by DFG grant No. BR 1084/4-1. Kind hospitality of the Kavli Institute for Theoretical Physics, Santa Barbara in the early stages of this project is gratefully acknowledged where parts of this work have been supported by NSF grant No. PHY99-07949.

- ¹ S. Chakravarty, B. I. Halperin, and D. R. Nelson, Phys. Rev. B **39**, 2344 (1989).
- ² A. V. Chubukov, S. Sachdev, and J. Ye, Phys. Rev. B **49**, 11919 (1994).
- ³ H. Tanaka, K. Takatsu, W. Shiramura, and T. Ono, J. Phys. Soc. Jpn. **65**, 1945 (1996).
- ⁴ K. Takatsu, W. Shiramura, and H. Tanaka, J. Phys. Soc. Jpn. **66**, 1611 (1997).
- ⁵ Y. Sasago, K. U. A. Zheludev, and G. Shirane, Phys. Rev. B **55**, 8357 (1997).
- ⁶ K. Goto, M. Fujisawa, Ono, Tanaka, and Y. Uwatoko, J. Phys. Soc. Jpn. **73**, 3254 (2004).
- ⁷ A. Oosawa, K. Kakurai, T. Osakabe, M. Nakamura, M. Takeda, and H. Tanaka, J. Phys. Soc. Jpn. **73**, 1446 (2004).
- ⁸ C. Rüegg, A. Furrer, D. Sheptyakov, T. Strässle, K. W. Krämer, H.-U. Güdel, and L. Mélési, Phys. Rev. Lett. **93**,

- 257201 (2004).
- ⁹ A. Oosawa, M. Ishii, and H. Tanaka, J. Phys.: Condens. Matter **11**, 265 (1999).
- ¹⁰ T. Nikuni, M. Oshikawa, A. Oosawa, and H. Tanaka, Phys. Rev. Lett. **84**, 5868 (2000).
- ¹¹ M. Jaime, V. F. Correa, N. Harrison, C. D. Batista, N. Kawashima, Y. Kazuma, G. A. Jorge, R. Stern, I. Heinmaa, S. A. Zvyagin, et al., Phys. Rev. Lett. **93**, 087203 (2004).
- ¹² M. Hase, I. Terasaki, Y. Sasago, K. Uchinokura, and H. Obara, Phys. Rev. Lett. **71**, 4059 (1993).
- ¹³ M. Azuma, Y. Fujishiro, M. Takano, M. Nohara, and H. Takagi, Phys. Rev. B **55**, R8658 (1997).
- ¹⁴ A. Oosawa, M. Fujisawa, K. Kakurai, and H. Tanaka, Phys. Rev. B **67**, 184424 (2003).
- ¹⁵ H. Fujiwara, Y. Shindo, and H. Tanaka, Prog. Theor. Phys. Suppl. **159**, 392 (2005).

- ¹⁶ G. B. Martins, E. Dagotto, and J. A. Riera, Phys. Rev. B **54**, 16032 (1996).
- ¹⁷ M. Sigrist and A. Furusaki, J. Phys. Soc. Jpn. **65**, 2385 (1996).
- ¹⁸ T. Miyazaki, M. Troyer, M. Ogata, K. Ueda, and D. Yoshioka, J. Phys. Soc. Jpn. **66**, 2580 (1997).
- ¹⁹ M. Laukamp, G. B. Martins, C. Gazza, A. L. Malvezzi, E. Dagotto, P. M. Hansen, A. C. López, and J. Riera, Phys. Rev. B **57**, 10755 (1998).
- ²⁰ S. Wessel, B. Normand, M. Sigrist, and S. Haas, Phys. Rev. Lett. **86**, 1086 (2001).
- ²¹ S. W. Cheong, A. S. Cooper, L. W. Rupp, B. Batlogg, J. D. Thompson, and Z. Fisk, Phys. Rev. Lett. **44**, 9739 (1991).
- ²² K. Kato, S. Todo, K. Harada, N. Kawashima, S. Miyashita, and H. Takayama, Phys. Rev. Lett. **84**, 4204 (2000).
- ²³ A. W. Sandvik, Phys. Rev. Lett. **86**, 3209 (2001).
- ²⁴ S. K. Ma, C. Dasgupta, and C. Hu, Phys. Rev. Lett. **43**, 1434 (1979).
- ²⁵ D. S. Fisher, Phys. Rev. B **50**, 3799 (1994).
- ²⁶ D. S. Fisher, Phys. Rev. B **51**, 6411 (1995).
- ²⁷ R. B. Griffiths, Phys. Rev. Lett. **23**, 17 (1969).
- ²⁸ A. W. Sandvik, Phys. Rev. Lett. **89**, 177201 (2002).
- ²⁹ O. P. Vajk and M. Greven, Phys. Rev. Lett. **89**, 177202 (2002).
- ³⁰ Y. C. Lin, H. Rieger, N. Laflorencie, and F. Igloi, *preprint: cond-mat/0604126*.
- ³¹ W. Brenig, Phys. Rev. B **73**, 104450 (2006).
- ³² W. Ling, K. S. D. Beach, and A. W. Sandvik, Phys. Rev. B **73**, 014431 (2006).
- ³³ A. W. Sandvik, Phys. Rev. B **59**, R14157 (1999).
- ³⁴ O. F. Syluåsen and A. Sandvik, Phys. Rev. E **66**, 046701 (2002).
- ³⁵ A. W. Sandvik, Phys. Rev. B **66**, 024418 (2002).
- ³⁶ A. W. Sandvik, E. Dagotto, and D. J. Scalapino, Phys. Rev. B **56**, 11701 (1997).
- ³⁷ A. Sokol, R. Glenister, and R. Singh, Phys. Rev. Lett. **72**, 1549 (1994).
- ³⁸ P. V. Shevchenko, A. W. Sandvik, and O. P. Sushkov, Phys. Rev. B **61**, 3475 (2000).